Supporting Information

New Indole Tubulin Assembly Inhibitors Cause Stable Arrest of Mitotic Progression, Enhanced Stimulation of Natural Killer Cell Cytotoxic Activity and Repression of Hedgehog-dependent Cancer

Giuseppe La Regina, Ruoli Bai, Antonio Coluccia, Valeria Famiglini, Sveva Pelliccia, Sara Passacantilli, Carmela Mazzoccoli, Vitalba Ruggieri, Annalisa Verrico, Andrea Miele, Ludovica Monti, Marianna Nalli, Romina Alfonsi, Lucia Di Marcotullio, Alberto Gulino, Biancamaria Ricci, Alessandra Soriani, Angela Santoni, Michele Caraglia, Stefania Porto, Eleonora Da Pozzo, Claudia Martini, Andrea Brancale, Luciana Marinelli, Ettore Novellino, Stefania Vultaggio, Mario Varasi, Ciro Mercurio, Giulio Dondio, Chiara Bigogno, Ernest Hamel, Patrizia Lavia, and Romano Silvestri

Contents

Figure 1S. Proposed binding mode of **10**, **18**, **28** and **44**.
Figure 2S. Proposed binding mode of **33** and **40**.
Figure 3S. Proposed binding mode of **40**.
Table 1S. Correlation docking score vs biological activity
Figure 4S. Correlation of MCF-7 cytotoxicity data with inhibition of tubulin assembly (A) and inhibition of colchicine binding (B).
Figure 5S. MDA-MB-468 cancer cell growth inhibition of by compound **33**.
Figure 6S. MDA-MB-436 cancer cell growth inhibition of by compound **33**.
Figure 7S. MDA-MB-231 cancer cell growth inhibition of by compound **33**.
Figure 8S. MDA-MB-468 cancer cell growth inhibition of by compound **44**.
Figure 9S. MDA-MB-436 cancer cell growth inhibition of by compound **44**.
Figure 10S. MDA-MB-231 cancer cell growth inhibition of by compound **44**.
Figure 11S. Cell cycle analysis of PC-3, RD and HepG2 cells treated with **33**, **44** or PTX for 24 h.
Figure 12S. Cell growth inhibition of **33**- or **44**-treated T98G cells.
Figure 13S. Cell growth inhibition of **33**- or **44**-treated U343 cells.
Figure 14S. Cell growth inhibition of ATI-treated HeLa cells after a 48 h treatment.
Figure 15S. mRNA abundance by real-time PCR after a 24 h treatment with the indicated ATI at 10 nM.
Figure 16S. Effects of ATI derivatives **33**, **44** and **81** on D283 cell growth.
Table 2S. Elemental Analysis of Compounds **6-45.**

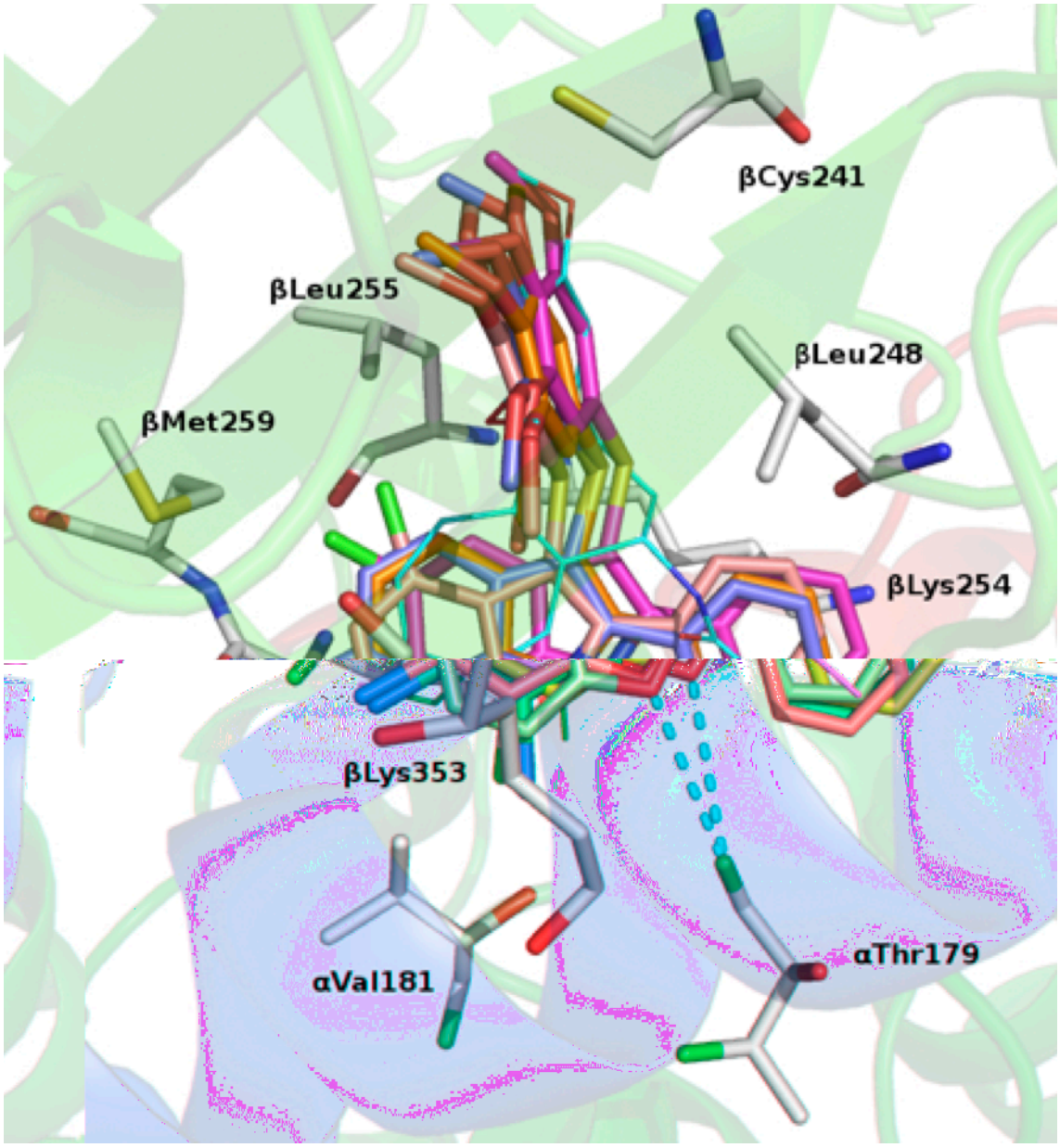

Figure 1S. Proposed binding mode of **10** (pink), **18** (magenta), **28** (violet), and **44** (orange); **1** is shown in cyan. Tubulin is represented as a cartoon for the α- (red) and β- (green) subunits. Residues forming interactions with the D region of the ATIs are depicted in white. Hydrogen bonds are indicated by yellow dashed lines.

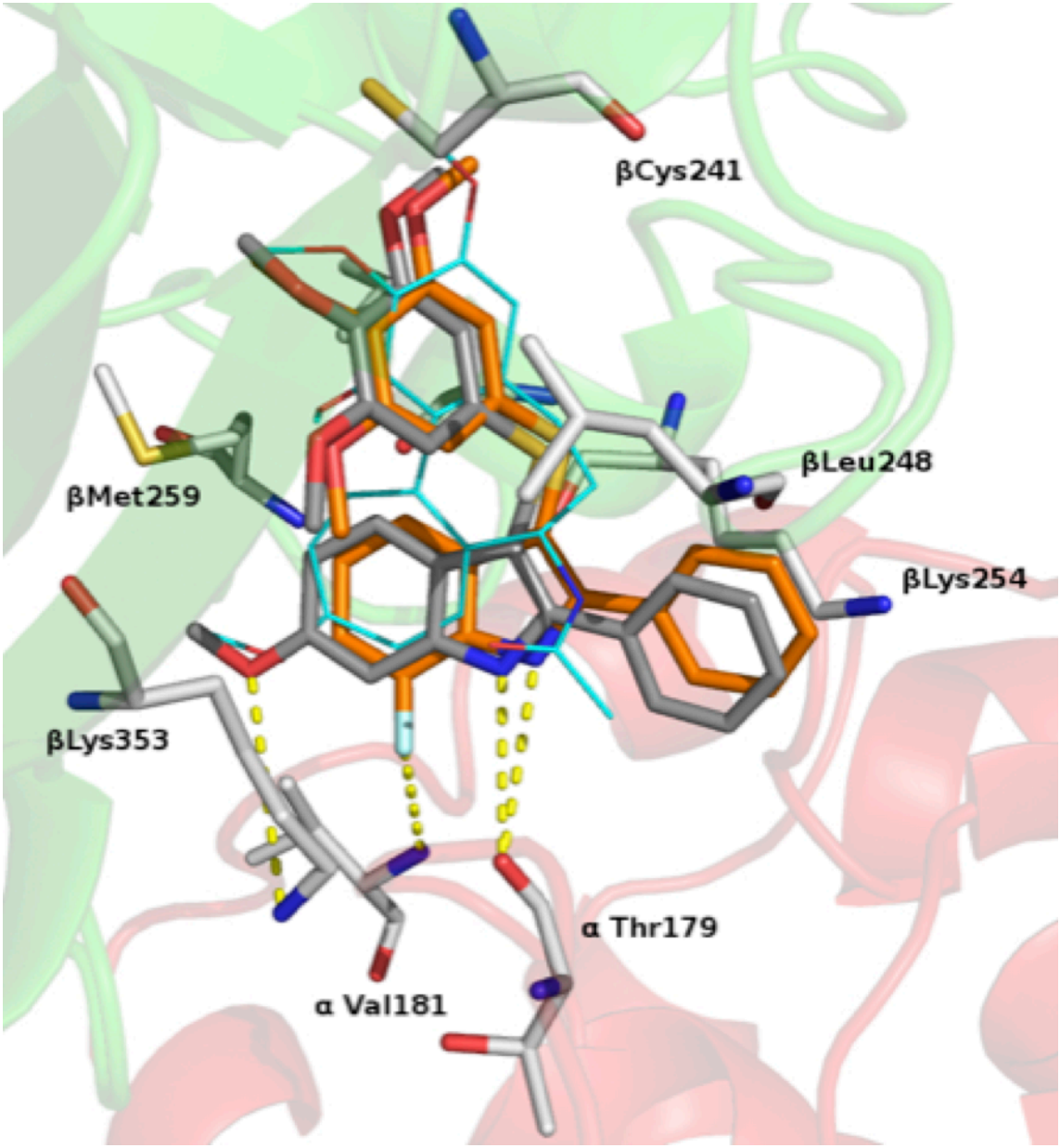

Figure 2S. Proposed binding modes of **33** (grey) and **40** (orange); **1** is shown in cyan. Tubulin is represented as a cartoon for the α- (red) and β- (green) subunits. Residues forming interactions with the D region of the ATIs are depicted in white. Hydrogen bonds are indicated by yellow dashed lines.

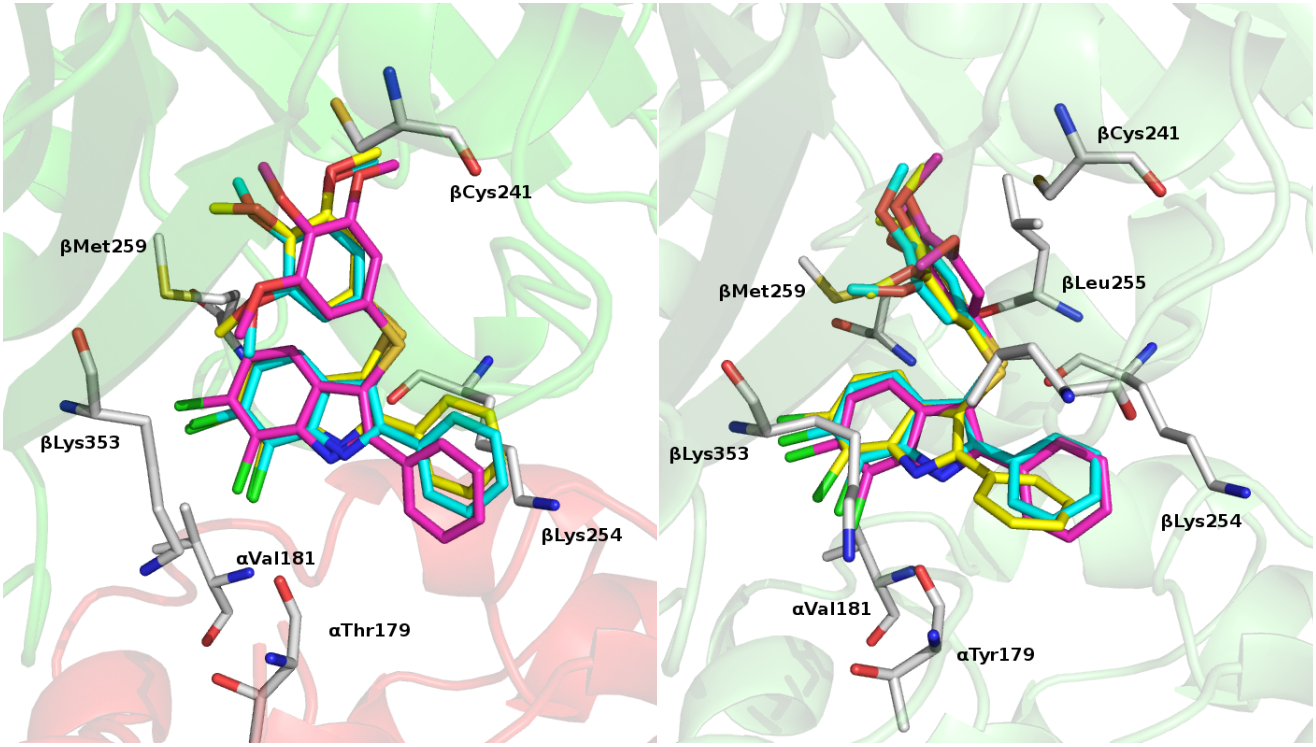

Figure 3S Left panel. Binding mode of **40** furnished by: PLANTS (cyan), Glide (magenta) and Autodock (yellow) versus 1SA0 tubulin crystal structure. Right panel. Binding mode of **40** furnished by: PLANTS (cyan), Glide (magenta) and Autodock (yellow) versus 42OA tubulin crystal structure.

Table 1S. Correlation docking score vs biological activity

	r^2	
Software	**1SA0**	**42OA**
Plants	0.03	0.05
Glide	0.02	0.03
Autodock	0.05	0.07

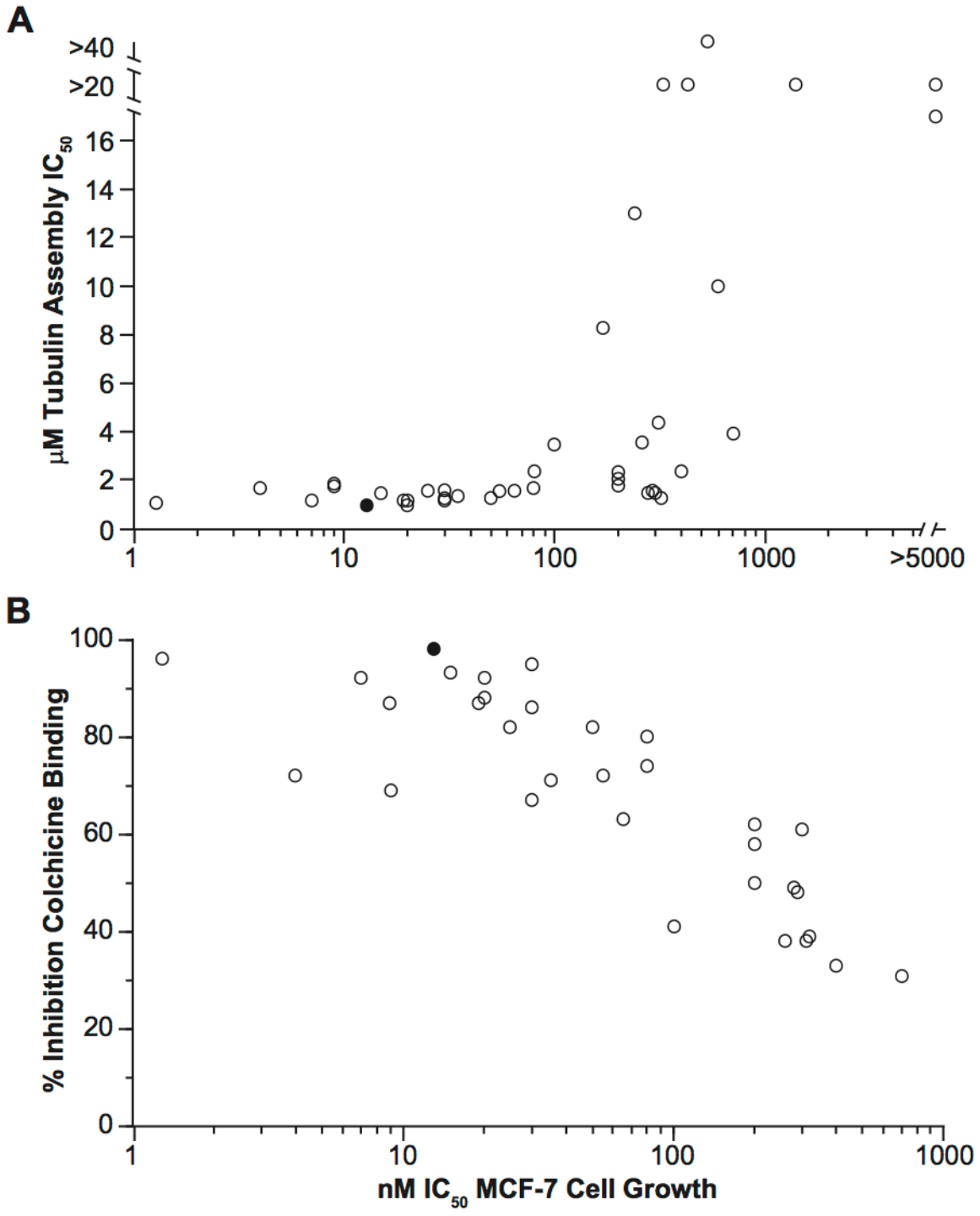

Figure 4S. Correlation of MCF-7 cytotoxicity data with inhibition of tubulin assembly (A) and inhibition of colchicine binding (B). Data of ATI derivatives **6-45** are shown as open circles. Black circle represents CSA4 as reference compound.

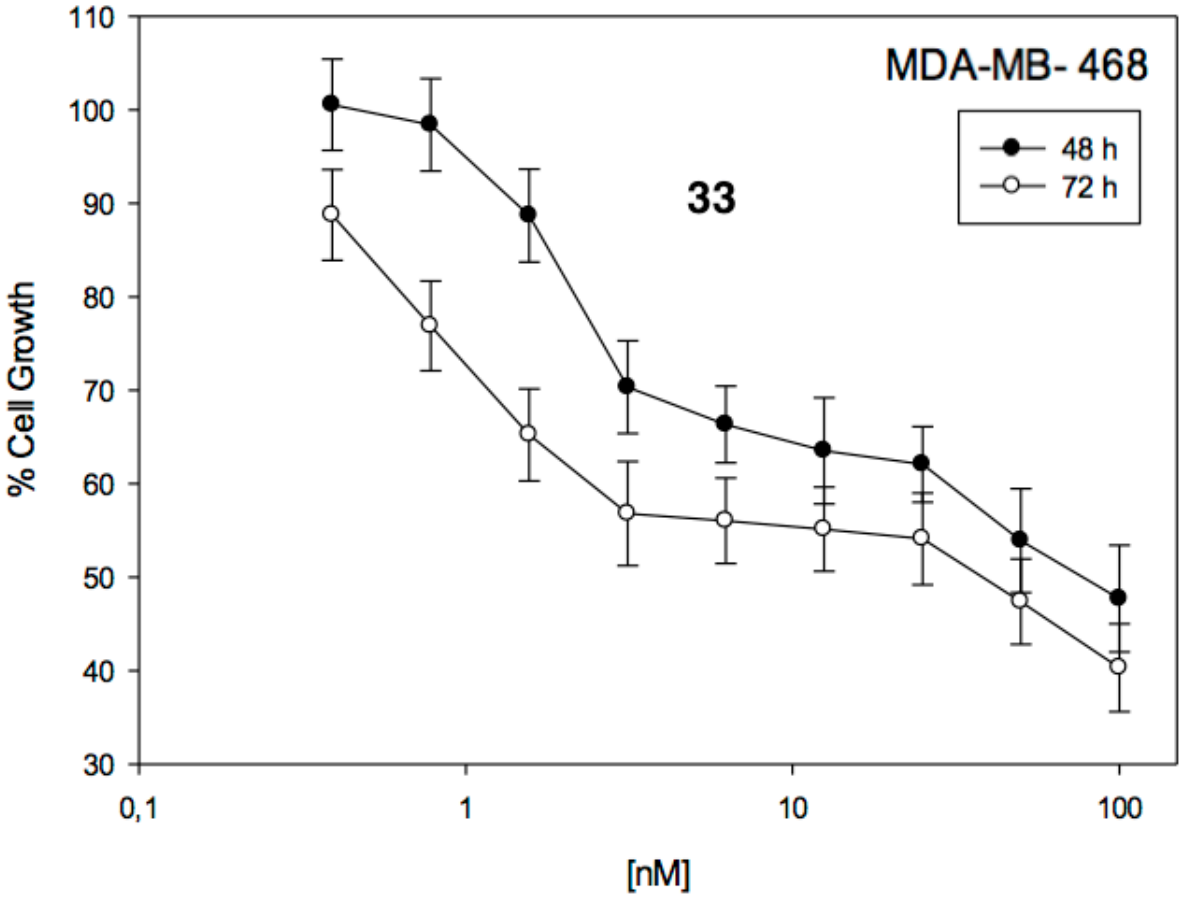

Figure 5S. MDA-MB-468 cancer cell growth inhibition of by compound **33**.

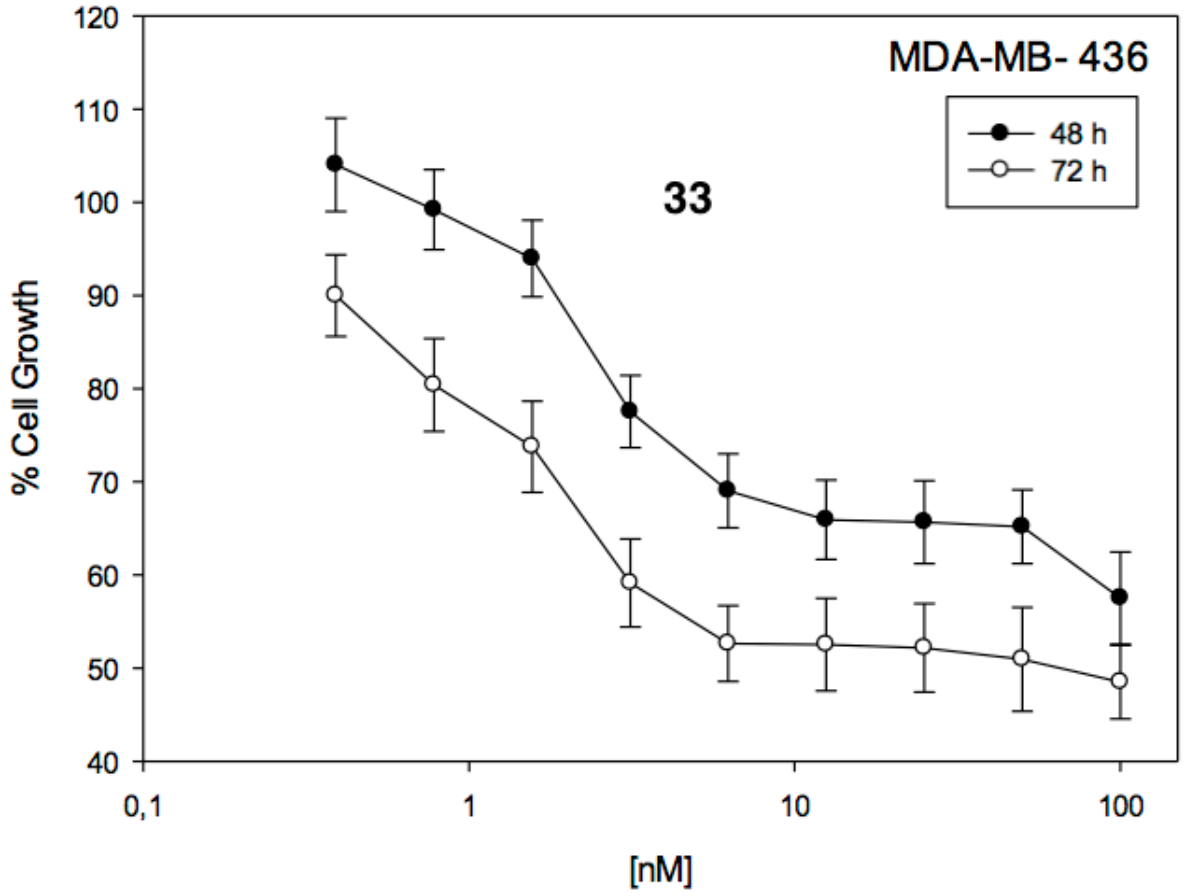

Figure 6S. MDA-MB-436 cancer cell growth inhibition of by compound **33**.

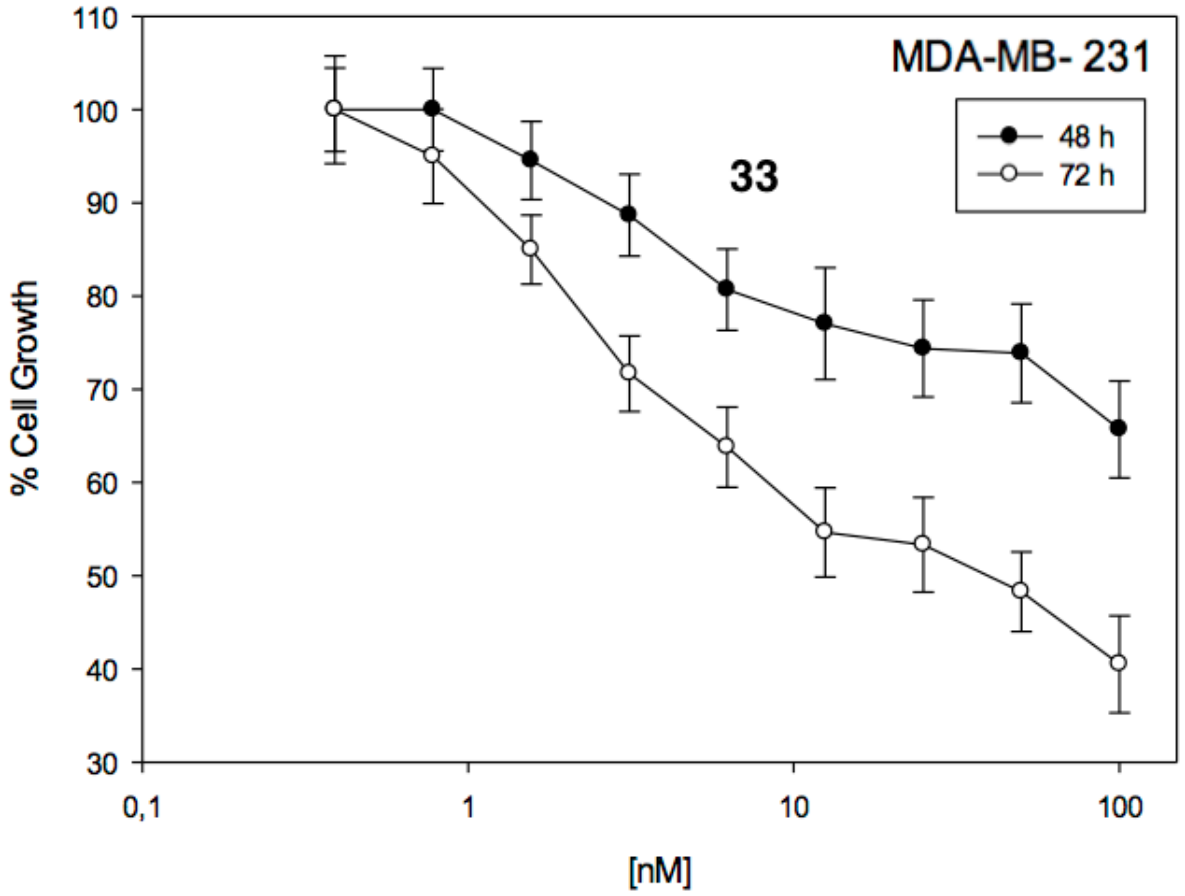

Figure 7S. MDA-MB-231 cancer cell growth inhibition of by compound **33**.

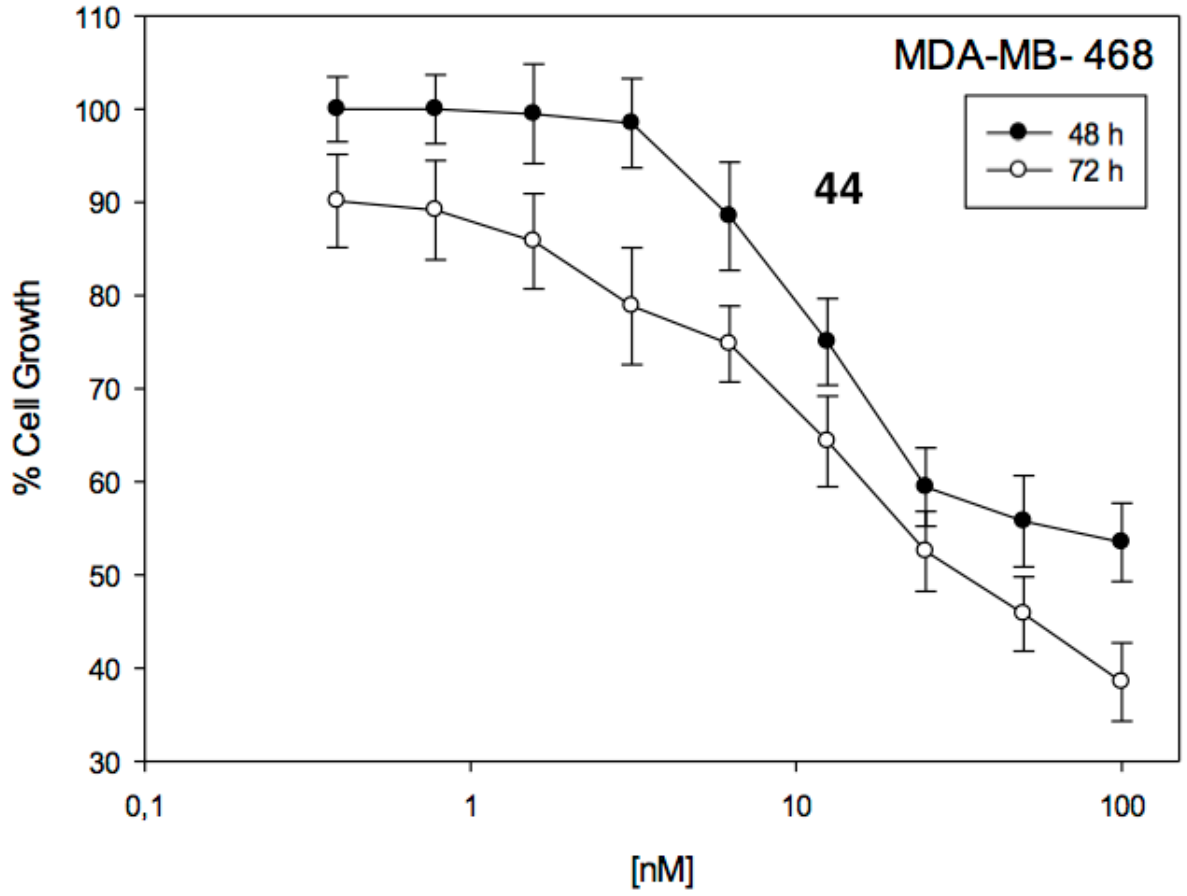

Figure 8S. MDA-MB-468 cancer cell growth inhibition of by compound **44**.

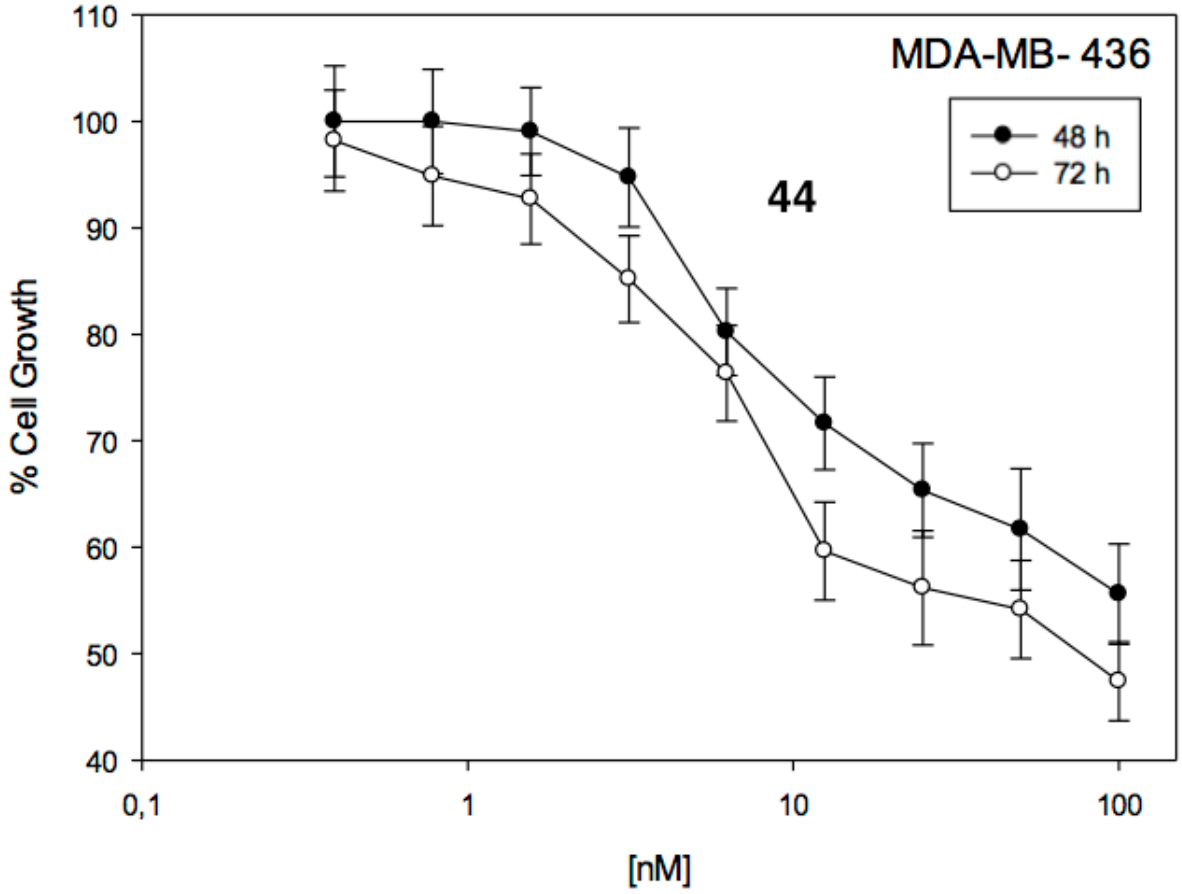

Figure 9S. MDA-MB-436 cancer cell growth inhibition of by compound **44**.

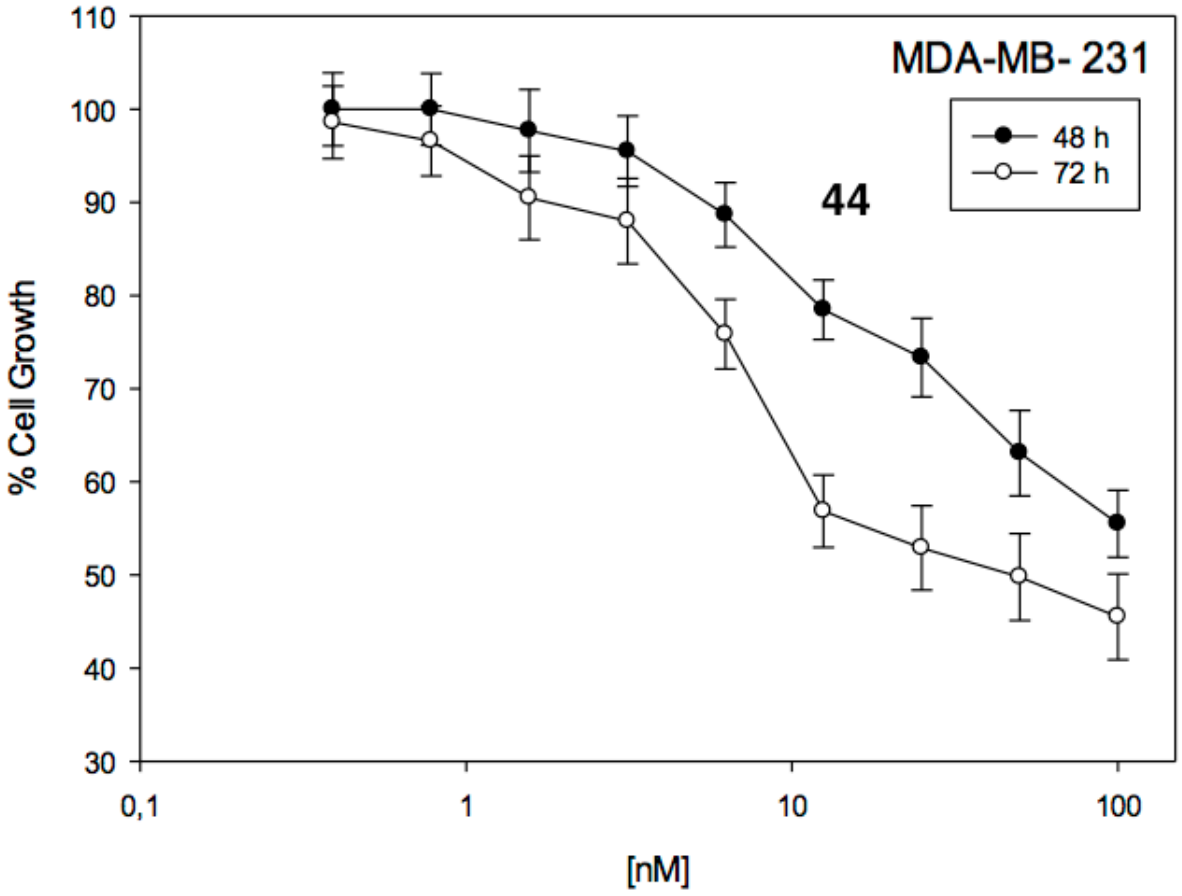

Figure 10S. MDA-MB-231 cancer cell growth inhibition of by compound **44**.

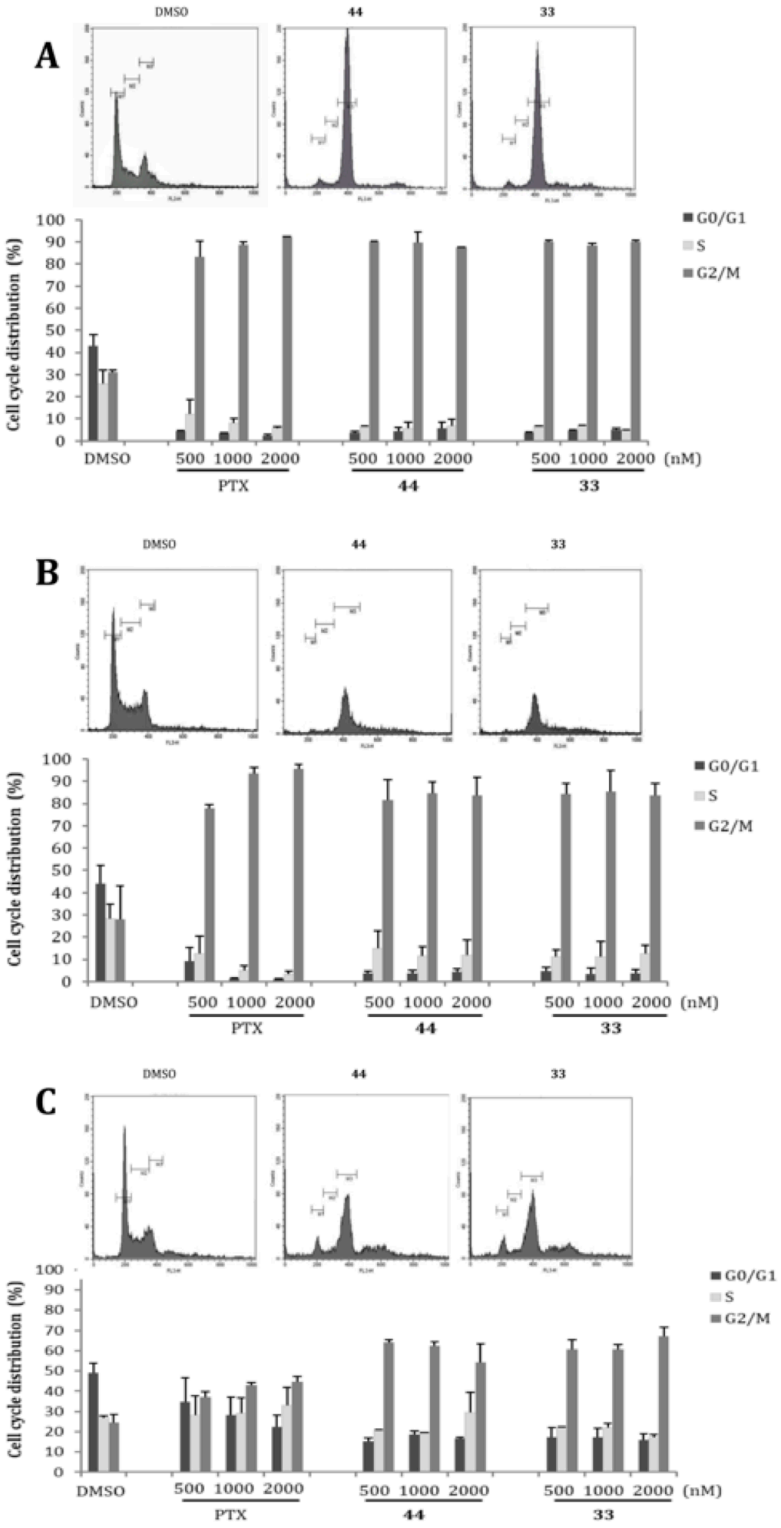

Figure 11S. Cell cycle analysis of PC-3 (A), RD (B) and HepG2 (C) cells treated with 0.1% DMSO or 500, 1000 or 2000 nM **33**, **44** or PTX for 24 h. Representative cell cycle profiles from cytometric analysis following treatment with 2000 nM **33** or **44** are shown at the top of each panel. Histograms represent % of cells with G0/G1, S and G2/M DNA content expressed as mean values ± SD of three independent experiments.

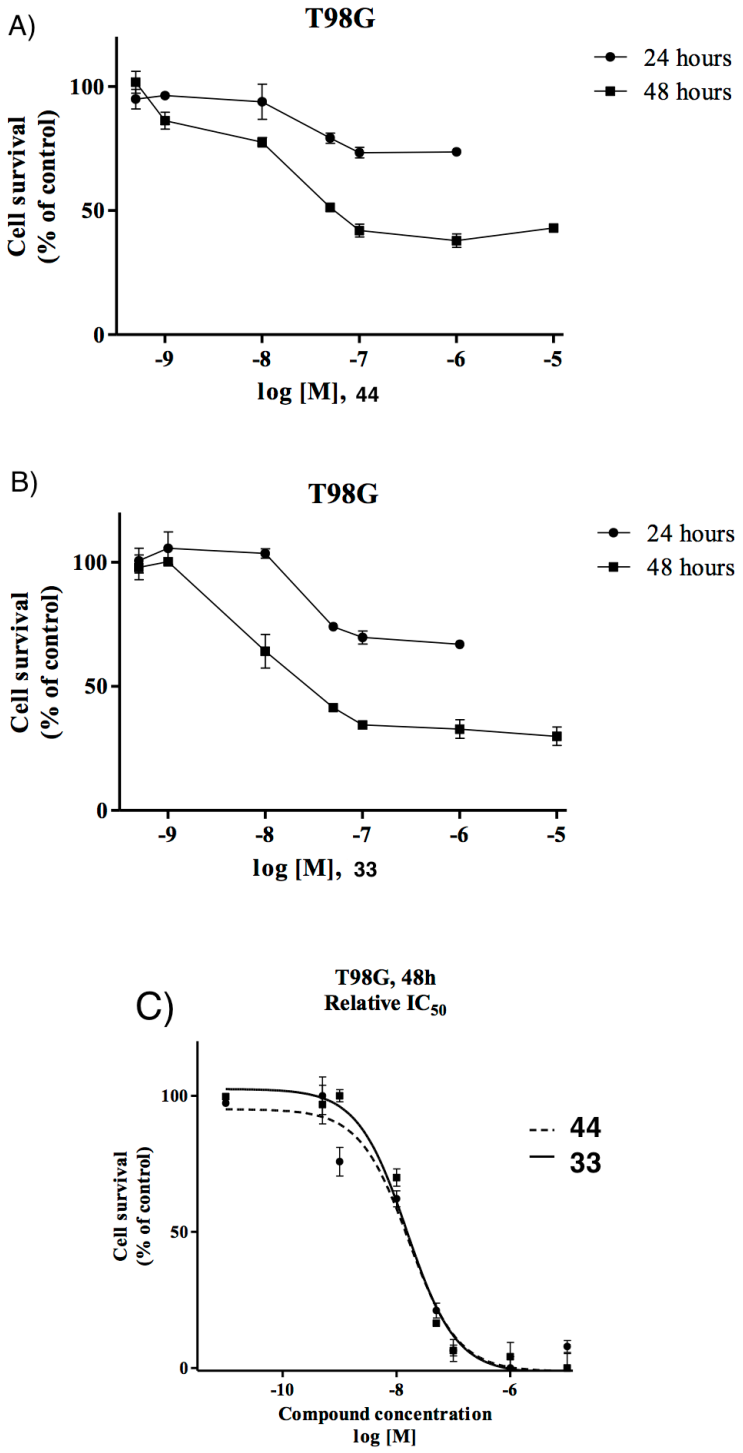

Figure 12S. Compounds **33** and **44** inhibit T98G cell growth/survival in a dose-dependent manner following a 24 (panel A) or 48 h (panel B) drug treatment. The % of **33-** and **44**-treated viable cells were calculated along with untreated control cells (value = 100%). Mean data ± SEM were obtained from 3 independent experiments performed in triplicate (*=p<0.05, **= p<0.01 and ***p<0.001, Oneway Anova, Bonferroni's corrected t-test for post-hoc pair-wise comparisons). In panel C, the relative IC_{50} curves are shown.

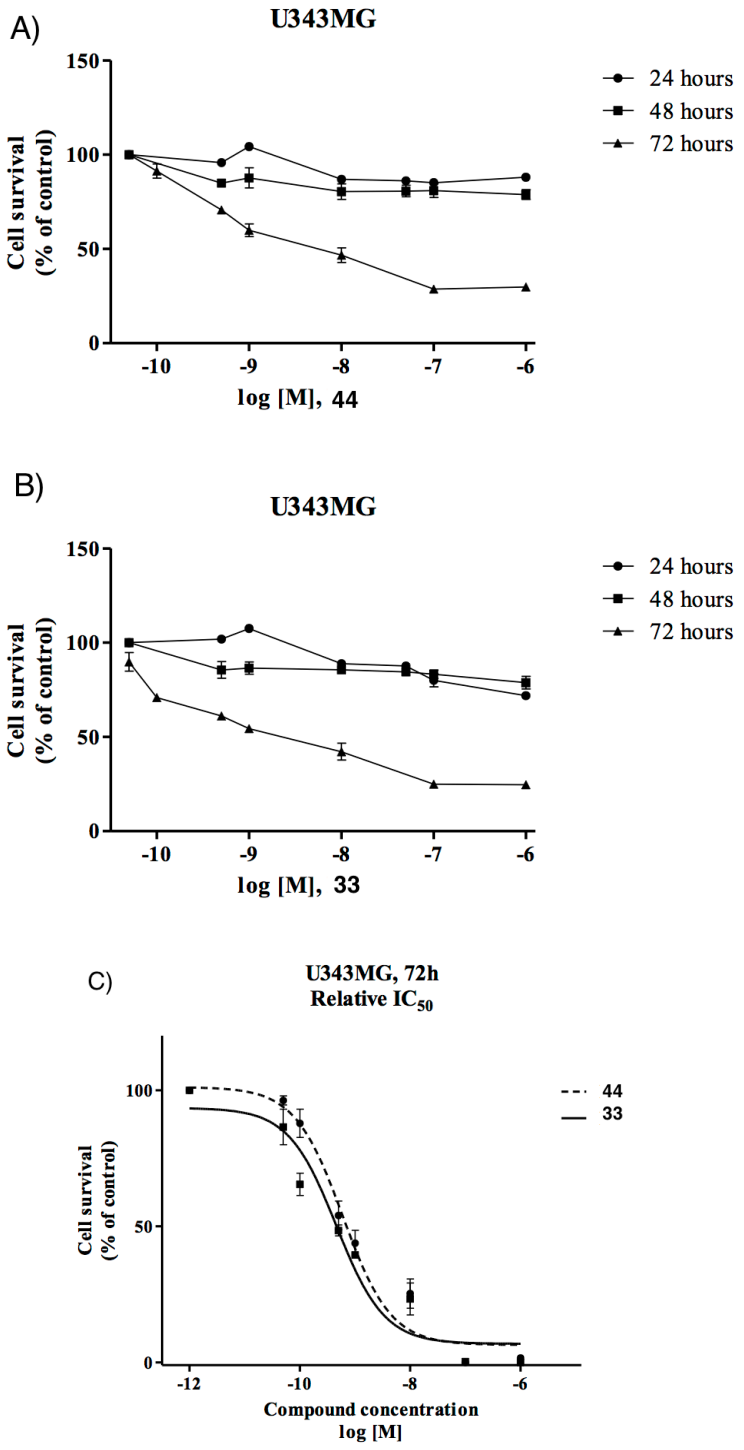

Figure 13S. Compounds **33** and **44** inhibit U343 cell growth/survival in a dose-dependent manner following a 24 (panel A), 48 (panel B) or 72 h (panel C) drug treatment. The % of **33-** and **44**-treated viable cells were calculated along with untreated control cells (value = 100%). Mean data ± SEM were obtained from 3 independent experiments performed in triplicate (*=p<0.05, **= p<0.01 and ***p<0.001, Oneway Anova, Bonferroni's corrected t-test for post-hoc pair-wise comparisons). In panel C, the relative IC_{50} curves are shown.

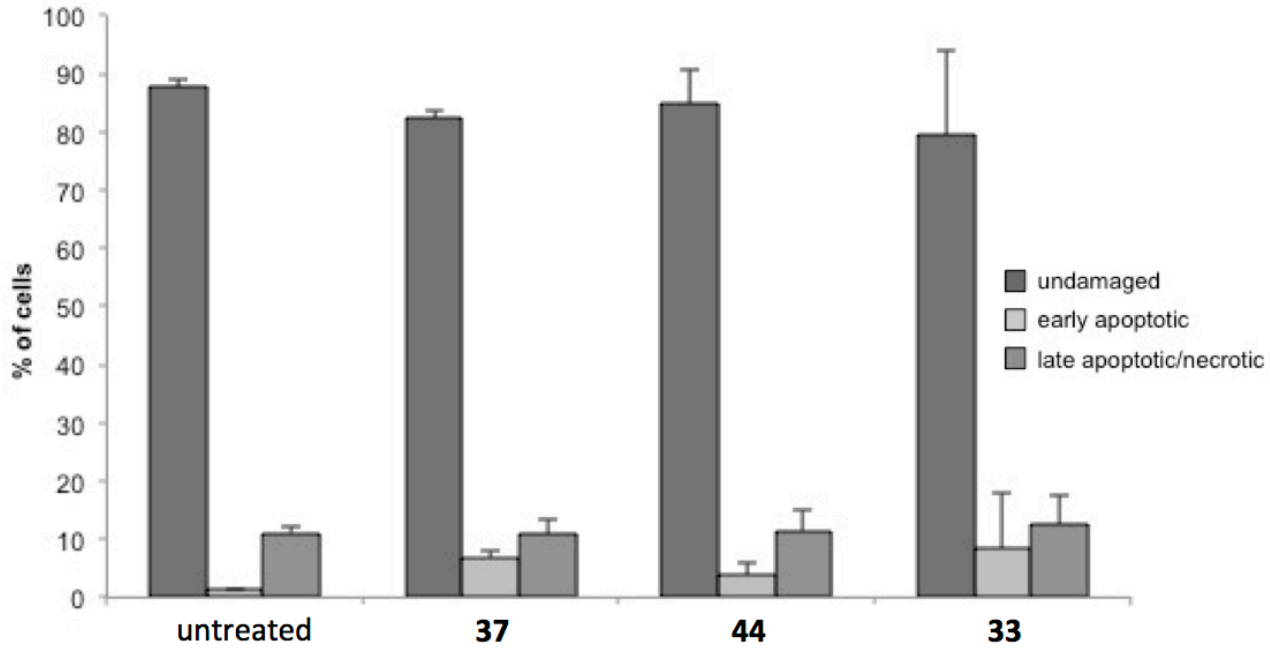

Figure 14S. Cell growth inhibition of HeLa cells after a 48 h treatment with ATI **37**, **44** or **33**.

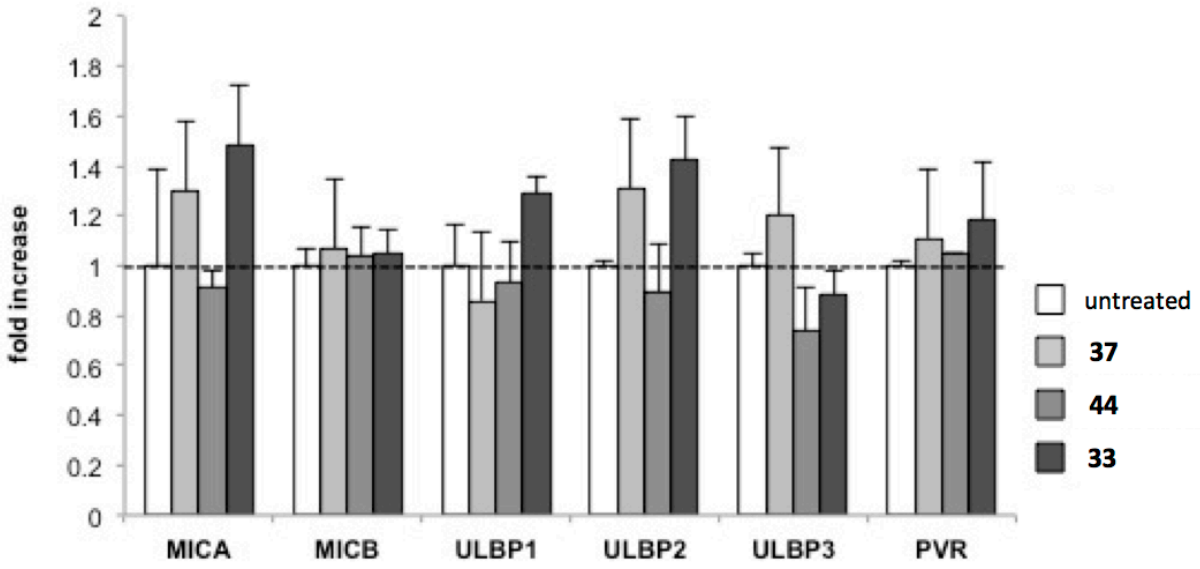

Figure 15S. mRNA abundance by real-time PCR after a 24 h treatment with the indicated ATI at 10 nM.

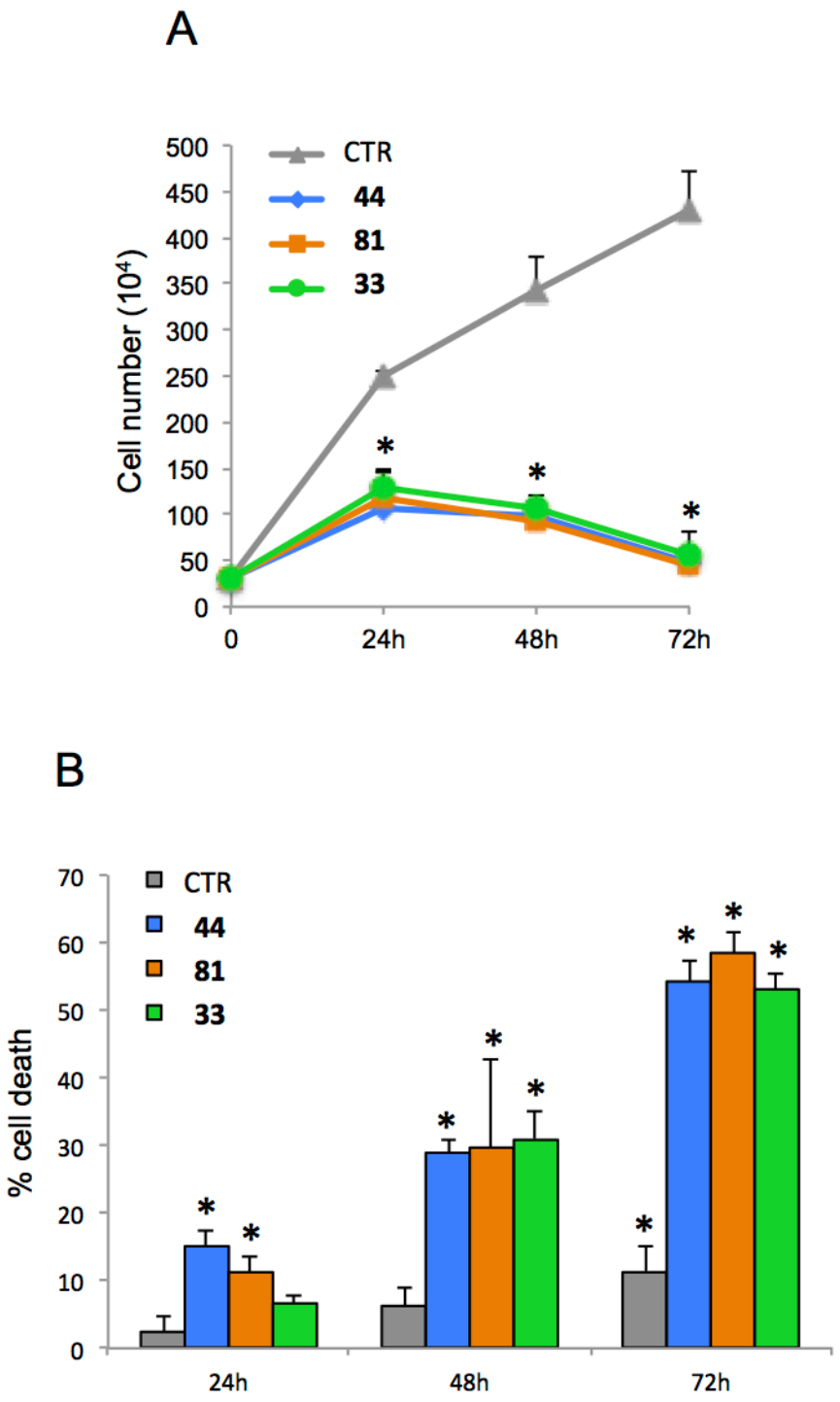

Figure 16S. Effect of ATI derivatives **33**, **44** and **81** on D283 cell growth. D283 cells were treated with these compounds (1 µM) or DMSO only, as control (CTR)**.** After the indicated times, a trypan blue count was performed to determine the growth rate (A) and the percentage of cell death (B). Data show the mean ± SD of three independent experiments. Error bars indicate SD. **P*, 0.05 vs CTR.

Table 2S. Elemental Analysis of Compounds 6-45.

compd	Elemental Analysis Calcd/Found
6	Calcd. for $C_{23}H_{20}BrNO_3S$: C, 58.73; H, 4.29; Br, 16.99; N, 2.98; S, 6.82. Found: C, 58.75; H, 4.31; Br, 16.99; N, 2.96; S, 6.85.
7	Calcd. for $C_{24}H_{20}BrNO_4$: C, 61.81; H, 4.32; Br, 17.13; N, 3.00. Found: C, 61.85; H, 4.29; Br, 17.13; N, 3.05.
8	Calcd. for $C_{23}H_{20}ClNO_3S$: C, 64.86; H, 4.73; Cl, 8.32; N, 3.29; S, 7.53. Found: C, 64.83; H, 4.76; Cl, 8.30; N, 3.28; S, 7.52.
9	Calcd. for $C_{24}H_{20}ClNO_4$: C, 68.33; H, 4.78; Cl, 8.40; N, 3.32. Found: C, 68.36; H, 4.81; Cl, 8.42; N, 3.36.
10	Calcd. for $C_{24}H_{22}ClNO_3$: C, 70.67; H, 5.44; Cl, 8.69; N, 3.43. Found: C, 70.62; H, 5.48; Cl, 8.69; N, 3.47.
11	Calcd. for $C_{23}H_{20}FNO_3S$: C, 67.46; H, 4.92; F, 4.64; N, 3.42; S, 7.83. Found: C, 67.50; H, 4.90; F, 4.66; N, 3.42; S, 7.85.
12	Calcd. for $C_{24}H_{20}FNO_4$: C, 71.10; H, 4.97; F, 4.69; N, 3.45. Found: C, 71.08; H, 4.99; F, 4.70; N, 3.46.
13	Calcd. for $C_{24}H_{23}NO_4S$: C, 68.39; H, 5.50; N, 3.32; S, 7.61. Found: C, 68.41; H, 5.47; N, 3.32; S, 7.60.
14	Calcd. for $C_{25}H_{23}NO_5$: C, 71.93; H, 5.55; N, 3.36. Found: C, 71.92; H, 5.50; N, 3.38.
15	Calcd. for $C_{23}H_{20}BrNO_3S$: C, 58.73; H, 4.29; Br, 16.99; N, 2.98; S, 6.82. Found: C, 58.77; H, 4.31; Br, 17.01; N, 2.98; S, 6.78.
16	Calcd. for $C_{24}H_{20}BrNO_4$: C, 61.81; H, 4.32; Br, 17.13; N, 3.00. Found: C, 61.79; H, 4.30; Br, 17.13; N, 3.06.
17	Calcd. for $C_{24}H_{22}BrNO_3$: C, 63.73; H, 4.90; Br, 17.66; N, 3.10. Found: C, 63.77; H, 4.92; Br, 17.70; N, 3.10.
18	Calcd. for $C_{23}H_{20}ClNO_3S$: C, 64.86; H, 4.73; Cl, 8.32; N, 3.29; S, 7.53. Found: C, 64.83; H, 4.73; Cl, 8.30; N, 3.29; S, 7.57.
19	Calcd. for $C_{24}H_{20}ClNO_4$: C, 68.33; H, 4.78; Cl, 8.40; N, 3.32. Found: C, 68.30; H, 4.77; Cl, 8.40; N, 3.35.
20	Calcd. for $C_{24}H_{22}ClNO_3$: C, 70.67; H, 5.44; Cl, 8.69; N, 3.43. Found: C, 70.65; H, 5.40; Cl, 8.71; N, 3.45.
21	Calcd. for $C_{23}H_{20}FNO_3S$: C, 67.46; H, 4.92; F, 4.64; N, 3.42; S, 7.83. Found: C, 67.49; H, 4.90; F, 4.60; N, 3.42; S, 7.85.
22	Calcd. for $C_{24}H_{20}FNO_4$: C, 71.10; H, 4.97; F, 4.69; N, 3.45. Found: C, 71.12; H, 4.95; F, 4.69; N, 3.47.
23	Calcd. for $C_{24}H_{23}NO_4S$: C, 68.39; H, 5.50; N, 3.32; S, 7.61. Found: C, 68.41; H, 5.50; N, 3.32; S, 7.59.
24	Calcd. for $C_{25}H_{23}NO_5$: C, 71.93; H, 5.55; N, 3.36. Found: C, 71.90; H, 5.55; N, 3.40.
25	Calcd. for $C_{25}H_{25}NO_4$: C, 74.42; H, 6.25; N, 3.47. Found: C, 74.39; H, 6.25; N, 3.50.

26 Calcd. for $C_{23}H_{20}BrNO_3S$: C, 58.73; H, 4.29; Br, 16.99; N, 2.98; S, 6.82.
Found: C, 58.77; H, 4.29; Br, 17.02; N, 2.98; S, 6.85.

27 Calcd. for $C_{24}H_{20}BrNO_4$: C, 61.81; H, 4.32; Br, 17.13; N, 3.00.
Found: C, 61.80; H, 4.35; Br, 17.15; N, 3.01.

28 Calcd. for $C_{23}H_{20}ClNO_3S$: C, 64.86; H, 4.73; Cl, 8.32; N, 3.29; S, 7.53.
Found: C, 64.90; H, 4.73; Cl, 8.29; N, 3.29; S, 7.53.

29 Calcd. for $C_{24}H_{20}ClNO_4$: C, 68.33; H, 4.78; Cl, 8.40; N, 3.32.
Found: C, 68.35; H, 4.78; Cl, 8.42; N, 3.30.

30 Calcd. for $C_{24}H_{22}ClNO_3$: C, 70.67; H, 5.44; Cl, 8.69; N, 3.43.
Found: C, 70.65; H, 5.44; Cl, 8.71; N, 3.43.

31 Calcd. for $C_{23}H_{20}FNO_3S$: C, 67.46; H, 4.92; F, 4.64; N, 3.42; S, 7.83.
Found: C, 67.50; H, 4.92; F, 4.60; N, 3.42; S, 7.86.

32 Calcd. for $C_{24}H_{20}FNO_4$: C, 71.10; H, 4.97; F, 4.69; N, 3.45.
Found: C, 71.08; H, 4.97; F, 4.72; N, 3.45.

33 Calcd. for $C_{24}H_{23}NO_4S$: C, 68.39; H, 5.50; N, 3.32; S, 7.61.
Found: C, 68.43; H, 5.50; N, 3.30; S, 7.61.

34 Calcd. for $C_{25}H_{23}NO_5$: C, 71.93; H, 5.55; N, 3.36.
Found: C, 71.90; H, 5.55; N, 3.40.

35 Calcd. for $C_{23}H_{20}BrNO_3S$: C, 58.73; H, 4.29; Br, 16.99; N, 2.98; S, 6.82.
Found: C, 58.75; H, 4.29; Br, 17.03; N, 2.98; S, 6.85.

36 Calcd. for $C_{24}H_{20}BrNO_4$: C, 61.81; H, 4.32; Br, 17.13; N, 3.00.
Found: C, 61.85; H, 4.29; Br, 17.13; N, 3.05.

37 Calcd. for $C_{23}H_{20}ClNO_3S$: C, 64.86; H, 4.73; Cl, 8.32; N, 3.29; S, 7.53.
Found: C, 64.90; H, 4.73; Cl, 8.29; N, 3.29; S, 7.49.

38 Calcd. for $C_{24}H_{20}ClNO_4$: C, 68.33; H, 4.78; Cl, 8.40; N, 3.32.
Found: C, 68.70; H, 4.78; Cl, 8.40; N, 3.35.

39 Calcd. for $C_{24}H_{22}ClNO_3$: C, 70.67; H, 5.44; Cl, 8.69; N, 3.43.
Found: C, 70.70; H, 5.42; Cl, 8.69; N, 3.46.

40 Calcd. for $C_{23}H_{20}FNO_3S$: C, 67.46; H, 4.92; F, 4.64; N, 3.42; S, 7.83.
Found: C, 67.50; H, 4.92; F, 4.60; N, 3.42; S, 7.86.

41 Calcd. for $C_{24}H_{20}FNO_4$: C, 71.10; H, 4.97; F, 4.69; N, 3.45.
Found: C, 71.09; H, 4.97; F, 4.70; N, 3.45.

42 Calcd. for $C_{24}H_{23}NO_4S$: C, 68.39; H, 5.50; N, 3.32; S, 7.61.
Found: C, 68.42; H, 5.50; N, 3.30; S, 7.61.

43 Calcd. for $C_{25}H_{23}NO_5$: C, 71.93; H, 5.55; N, 3.36.
Found: C, 71.90; H, 5.55; N, 3.31.

44 Calcd. for $C_{23}H_{19}Cl_2NO_3S$: C, 60.00; H, 4.16; Cl, 15.40; N, 3.04; S, 6.97.
Found: C, 60.05; H, 4.14; Cl, 15.43; N, 3.04; S, 7.01.

45 Calcd. for $C_{24}H_{19}Cl_2NO_4S$: C, 63.17; H, 4.20; Cl, 15.54; N, 3.07.
Found: C, 63.15; H, 4.19; Cl, 15.50; N, 3.05.